Supplementary

Table S1 TP53 status of cell lines

Cell lines	p53 status
A549	WT
NCL-H1299	WT
NCL-H1975	Mutant p53 Arg273His
PC9	Mutant p53 Arg248Gln
NCL-H23	Mutant p53 Met246Ile
HCC827	Mutant p53 Val218del
NCL-H1650	Missense mutation of p53

WT, wild-type.

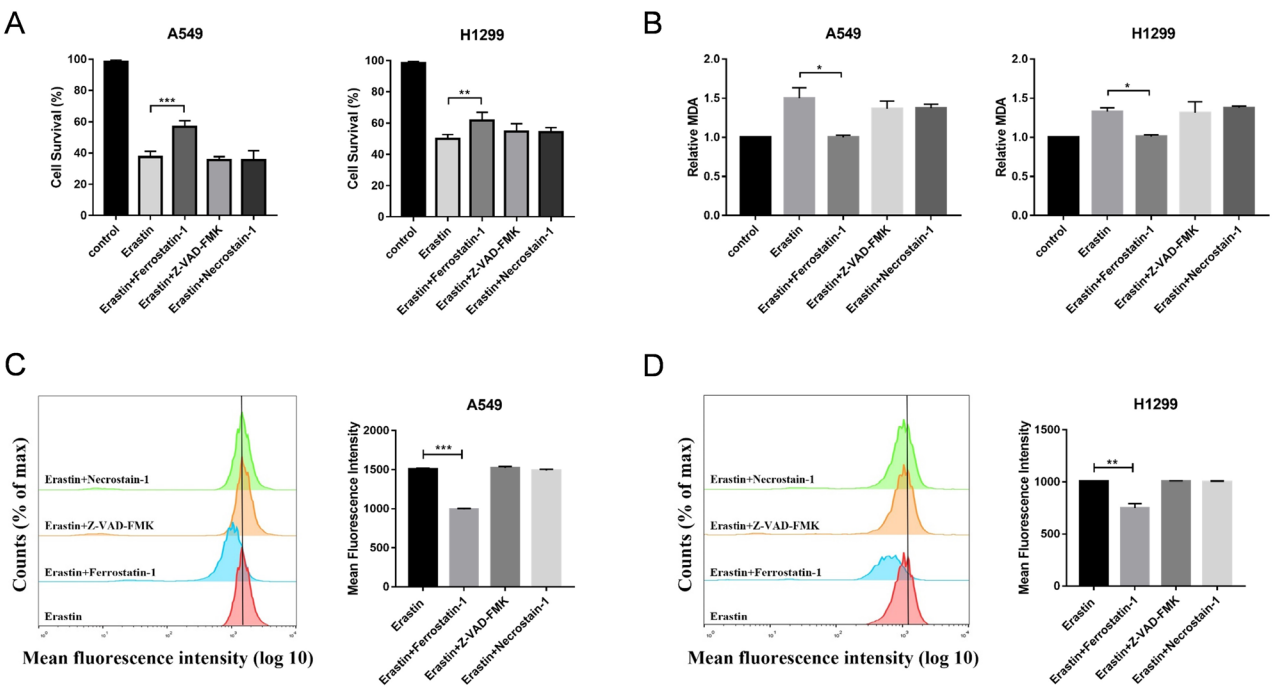

Figure S1 Erastin can specifically induce LUAD cell ferroptotic death. (A) A CCK-8 assay was used to analyze cell viability. (B) MDA levels within cells were quantified. (C,D) Increased levels of ROS in cells were analyzed using flow cytometry, with FlowJo being used to analyze the results. *, P<0.05; **, P<0.01; ***, P<0.001 *vs.* corresponding NC group. Data are representative findings for three independent experimental replicates and are given as the mean ± SD. MDA, malondialdehyde; LUAD, lung adenocarcinoma; CCK-8, Cell Counting Kit-8; ROS, reactive oxygen species; NC, negative control; SD, standard deviation.

https://dx.doi.org/10.21037/tlcr-24-762

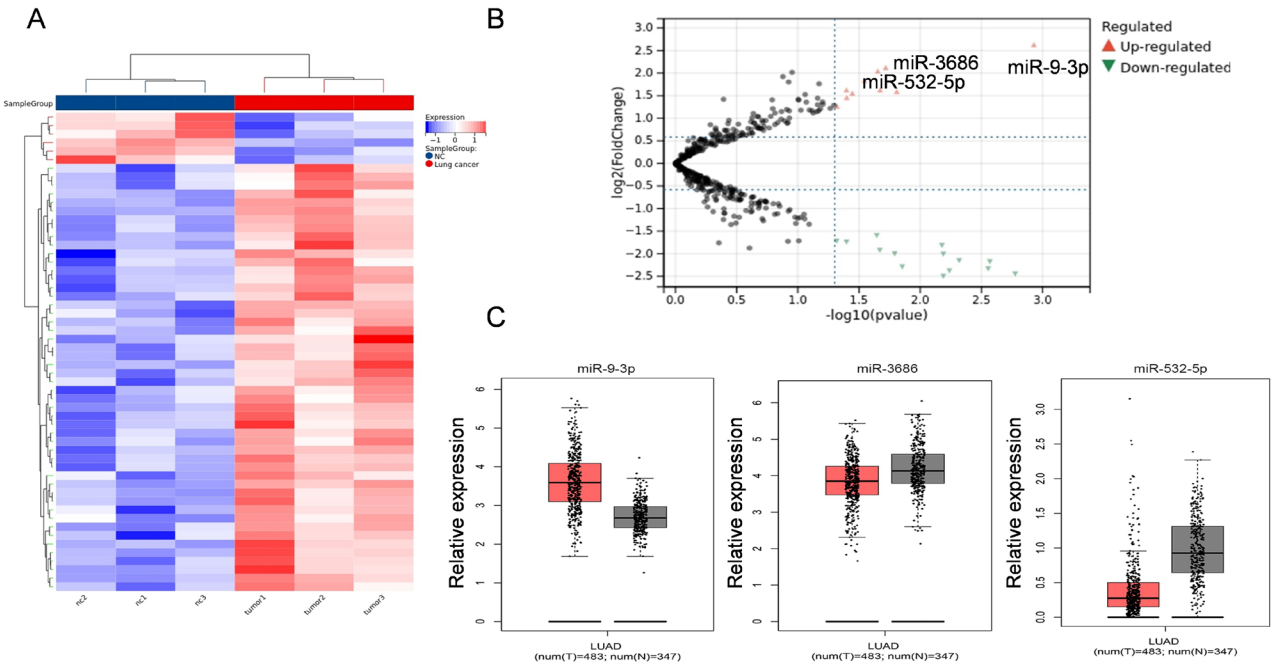

Figure S2 MiR-9-3p was differentially expressed in LUAD. (A,B) Cluster heatmap and volcano map showing the differential expression of miRNAs. (C) TCGA database was used to predict miRNAs expression in tissue samples from patients with LUAD. (D) Correlation of these six genes with miR-9-3p in LUAD tumor tissue samples. NC, negative control; LUAD, lung adenocarcinoma; T, tumor; N, normal; miRNA, microRNA; TCGA, The Cancer Genome Atlas.

https://dx.doi.org/10.21037/tlcr-24-762

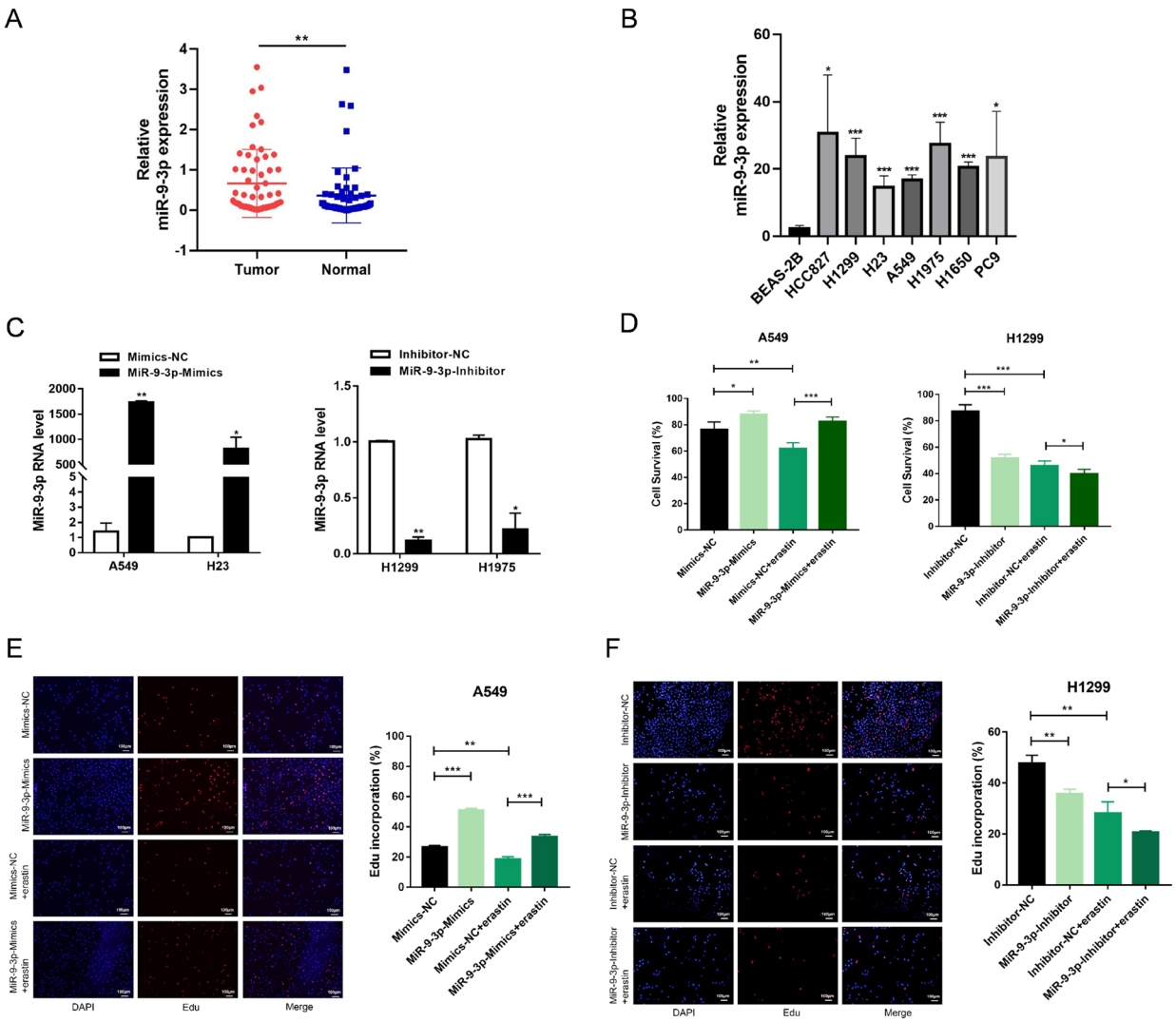

Figure S3 MiR-9-3p inhibition results in more pronounced inhibition of LUAD cell proliferation in response to erastin treatment. (A,B) MiR-9-3p expression was analyzed via qPCR in LUAD tissue samples and cell lines. (C) MiR-9-3p mimic or inhibitor transfection efficiency was analyzed via qPCR in LUAD cells. (D) A CCK-8 assay was used to evaluate the impact of miR-9-3p inhibitor or mimic transfection and erastin treatment on LUAD cell viability. (E,F) LUAD cell proliferation following miR-9-3p knockdown or overexpression and erastin treatment was assessed through EdU assays. *, P<0.05; **, P<0.01; ***, P<0.001 *vs.* corresponding NC group. Data are representative findings for three independent experimental replicates and are given as the mean ± SD. NC, negative control; DAPI, 4',6-diamidino-2-phenylindole; EdU, 5-ethynyl-2'-deoxyuridine; LUAD, lung adenocarcinoma; qPCR, quantitative polymerase chain reaction; CCK-8, Cell Counting Kit-8; SD, standard deviation.

https://dx.doi.org/10.21037/tlcr-24-762

Table S2 Relationship of miR-9-3p expression with clinicopathological features in patients with LUAD

Characteristics	Cases (n=60)	miR-9-3p expression		P value
		Low (n=30)	High (n=30)	
Age (years)				0.60
≤60	23	10	13	
>60	37	20	17	
Sex				0.60
Male	23	13	10	
Female	37	17	20	
Tumor size (cm)				0.002**
<5	29	21	8	
≥5	31	9	22	
Tumor differentiation				0.44
Well + moderate	30	17	13	
Poor	30	13	17	
Lymphatic metastasis				0.60
No	35	19	16	
Yes	25	11	14	
TNM stage				0.75
I-II	48	25	23	
III-IV	12	5	7	
Smoking status				0.57
Smoker	17	7	10	
Never-smoker	43	23	20	
Serum proGRP (pg/mL)				0.36
≤50	46	25	21	
>50	14	5	9	
Serum Cyfra21-1 (ng/mL)				0.67
≤3.3	54	26	28	
>3.3	6	4	2	
Serum NSE (ng/mL)				0.47
≤16	51	24	27	
>16	9	6	3	
Serum CEA (ng/mL)				0.53
≤5	47	25	22	
>5	13	5	8	
Serum SCC (ng/mL)				0.20
<1.5	54	25	29	
≥1.5	6	5	1	

**, P<0.01. LUAD, lung adenocarcinoma; TNM, tumor-node-metastasis; proGRP, progastrin-releasing peptide; Cyfra21-1, cytokeratin 19 fragment; NSE, neuron-specific enolase; CEA, carcinoembryonic antigen; SCC, squamous cell carcinoma.

https://dx.doi.org/10.21037/tlcr-24-762

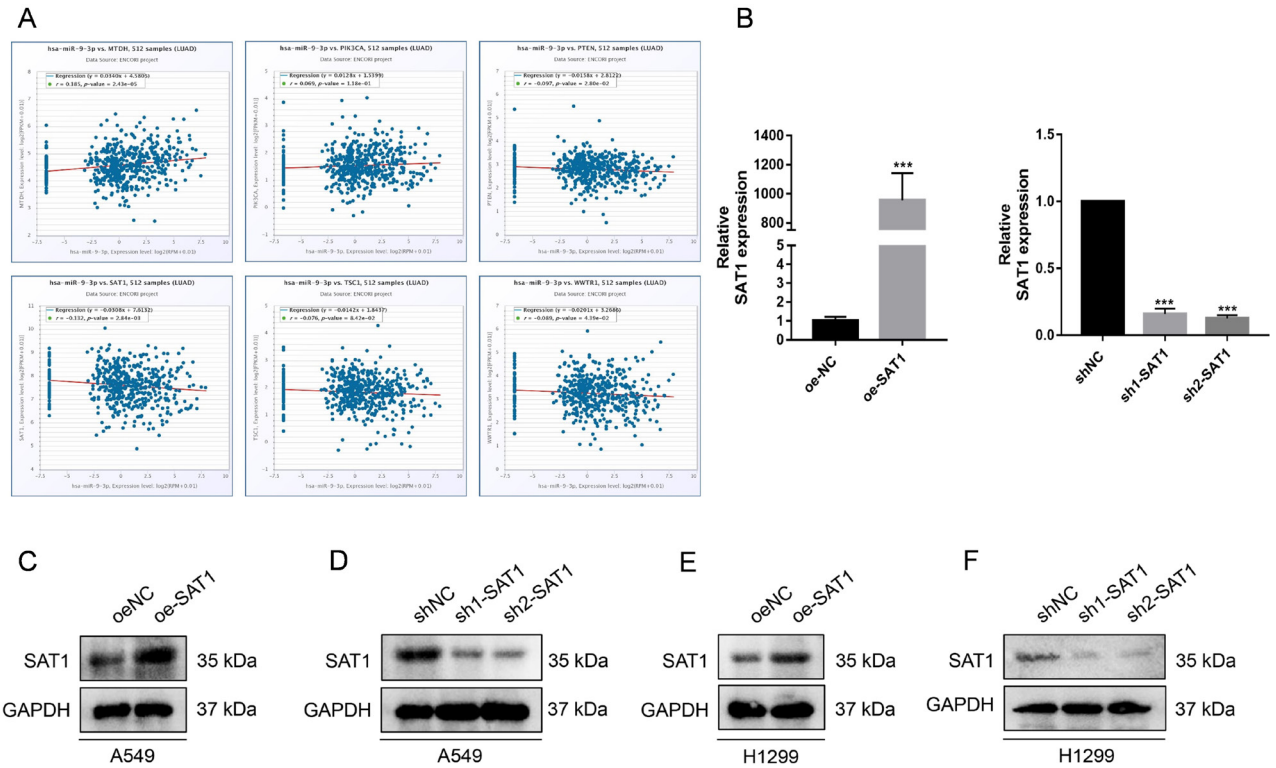

Figure S4 Knockdown and overexpression of SAT1 were expressed efficiently in LUAD cells. (A) Correlation of these six genes with miR-9-3p in LUAD tumor tissue samples. (B-F) qPCR and western blot were used to verify the efficiency of shRNA (sh1-SAT1 or sh2-SAT1) and SAT1 overexpression constructs in LUAD cells. ***, P<0.001 *vs.* corresponding NC group. Data are representative findings for three independent experimental replicates and are given as the mean ± SD. LUAD, lung adenocarcinoma; RPM, reads per million; oe, overexpression; NC, negative control; SAT1, spermidine/spermine N1-acetyltransferase 1; sh, short hairpin; GAPDH, glyceraldehyde 3-phosphate dehydrogenase; qPCR, quantitative polymerase chain reaction; SD, standard deviation.

https://dx.doi.org/10.21037/tlcr-24-762

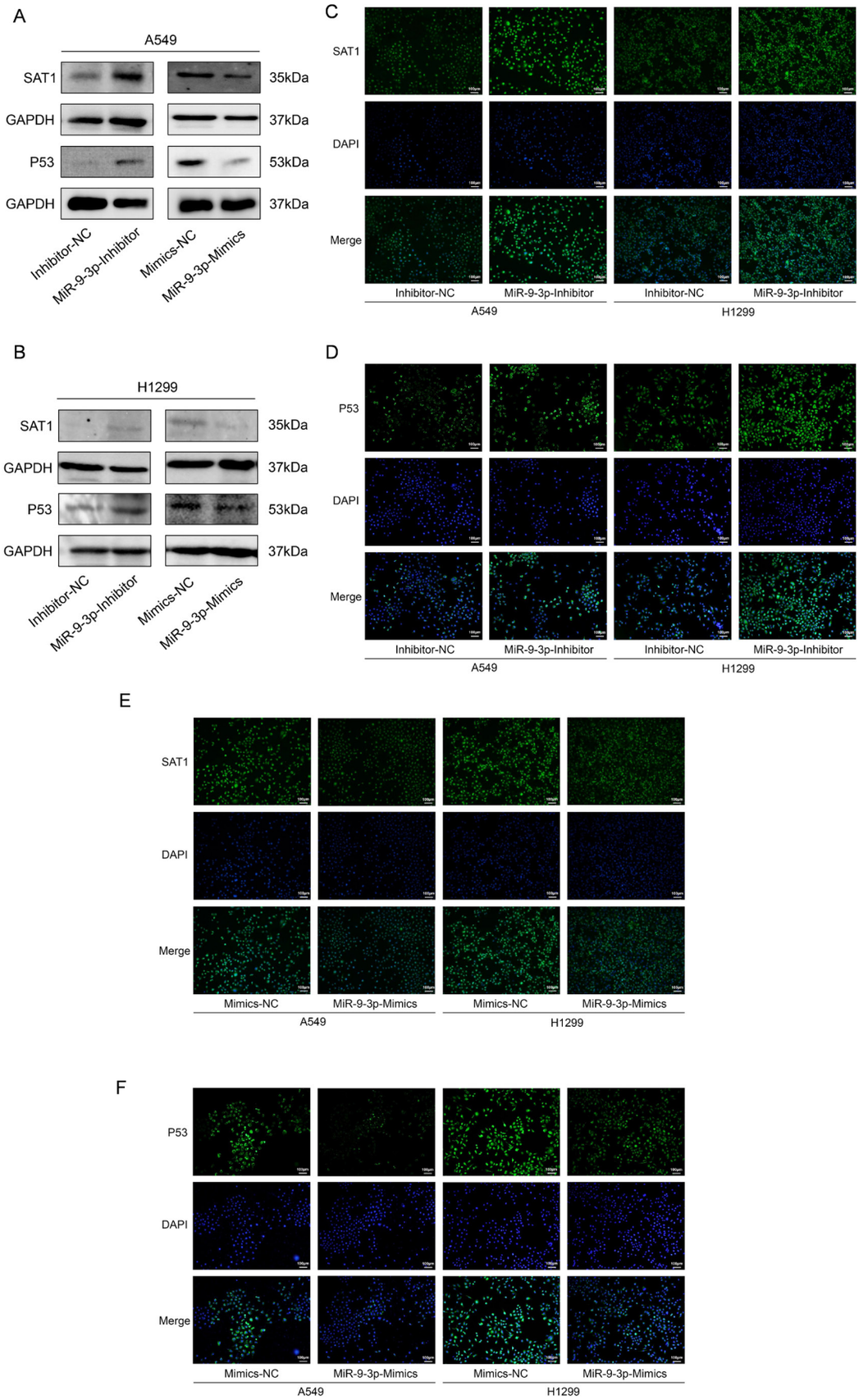

Figure S5 MiR-9-3p binds SAT1 to regulate p53. (A,B) P53 and SAT1 expression levels in H1299 and A549 with miR-9-3p-mimics or inhibitor were analyzed via Western blotting. (C-F) Detection of p53 and SAT1 expression levels by cell immunofluorescence assay. The cells were stained with antibodies for SAT1 and P53 and the nucleus was labeled with DAPI. Scale bar, 100 μm. SAT1, spermidine/spermine N1-acetyltransferase 1; GAPDH, glyceraldehyde 3-phosphate dehydrogenase; NC, negative control; DAPI, 4',6-diamidino-2-phenylindole.

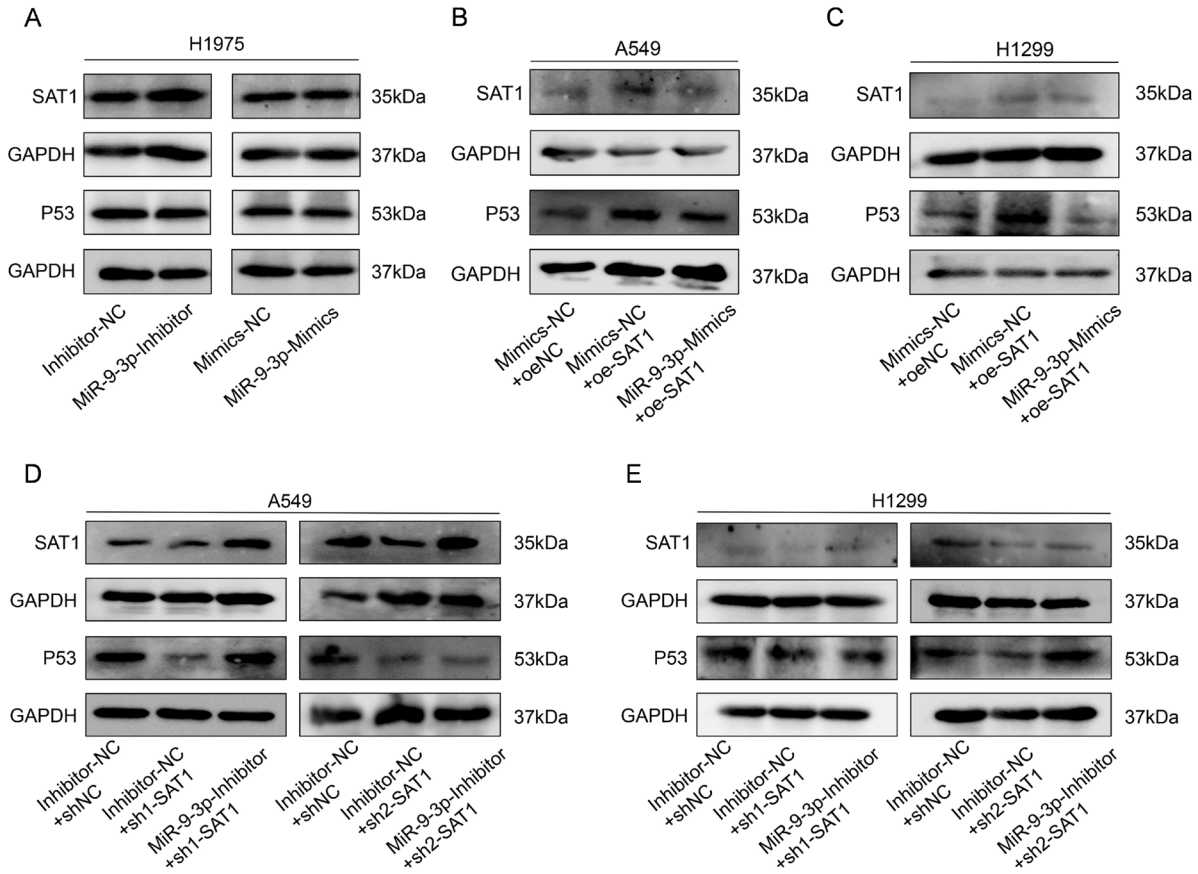

Figure S6 Western blotting in the recovery experiment. (A) The effect of miR-9-3p-mimics or inhibitor on the expression of p53 and SAT1 in H1975 cells detected by Western blotting. (B-E) The expression of p53 and SAT1 in the recovery experiment was detected by Western blot. SAT1, spermidine/spermine N1-acetyltransferase 1; GAPDH, glyceraldehyde 3-phosphate dehydrogenase; NC, negative control; oe, overexpression; sh, short hairpin.

https://dx.doi.org/10.21037/tlcr-24-762

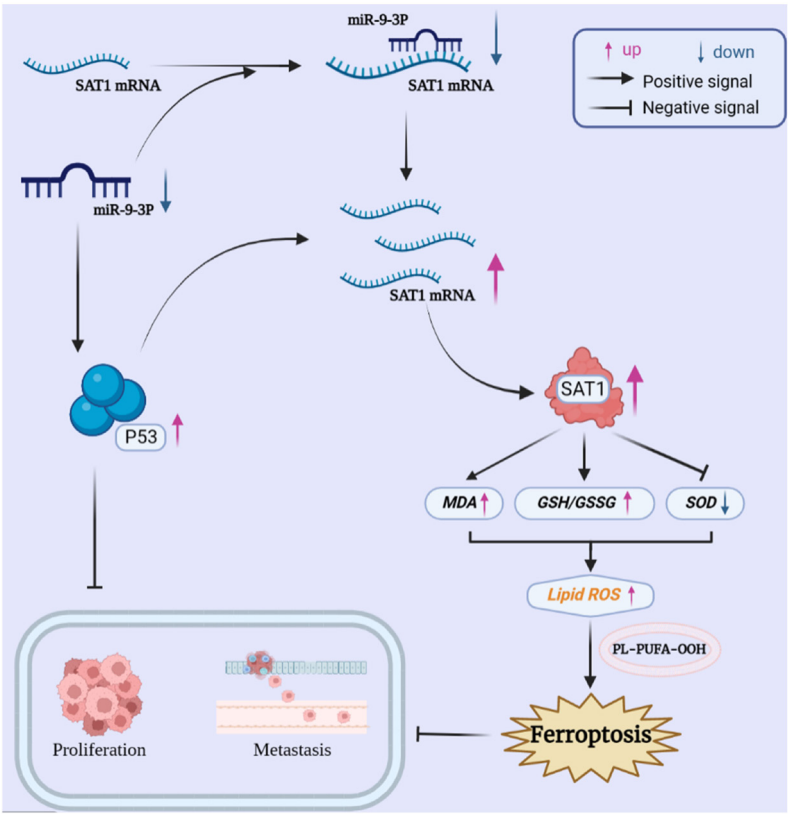

Figure S7 The p53 signaling pathway inhibits the miR-9-3p/SAT1-mediated regulation of LUAD cell ferroptosis. Functionally, miR-9-3p can target SAT1, thereby controlling the proliferation, metastatic progression, and ferroptotic death of LUAD cells through a pathway that depends on p53 signaling. SAT1, spermidine/spermine N1-acetyltransferase 1; mRNA, messenger RNA; MDA, malondialdehyde; GSH, glutathione; GSSG, oxidized glutathione; SOD, superoxide dismutase; ROS, reactive oxygen species; LUAD, lung adenocarcinoma.

https://dx.doi.org/10.21037/tlcr-24-762